DOI: 10.2507/33rd.daaam.proceedings.xxx

OPTIMAL CONTROL OF THE DC MOTOR IN THE TUNING OF THE SPACE-BASED REFLECTOR OF THE RADAR-REFLECTING NETTING

Fedor Mitin & Alexey Krivushov

This Publication has to be referred as: Mitin, F[edor]; Krivushov, A[lexey] (2022). Optimal control of the DC motor in the tuning of the space-based reflector of the radar-reflecting netting, Proceedings of the 33rd DAAAM International Symposium, pp.xxxx-xxxx, B. Katalinic (Ed.), Published by DAAAM International, ISBN 978-3-902734-xx-x, ISSN 1726-9679, Vienna, Austria
DOI: 10.2507/33rd.daaam.proceedings.xxx

Abstract

This paper discusses the DC motor control applied to a large-sized transformable reflector when tuning a radar-reflecting netting. For technology used in outer space, energy efficiency is an important indicator. For large-sized structures, additional requirements are set to minimize the structural vibration. Fluctuations in the active surface of the reflector's netting affect the directivity diagram, so the radar-reflective form must be adjusted gradually. This paper investigates the possibility of minimizing the energy costs of motor control by applying real-time optimal control algorithms. Numerical simulation results showing the possibility of using the proposed algorithm are presented. The problem of exact fulfillment of terminal conditions is solved. The study results allow control optimization for different types of DC motors.

Keywords: DC motor; optimal control; energy costs; space-based reflector; radar-reflecting netting.

1. Introduction

Electric motors, in view of their purpose, namely the conversion of electrical energy into mechanical energy, have found their application in products from various industries: from industrial machines to the space industry [1], [2], [3], [4], [5].

When choosing of the electric motor for products of space products for use as a part of actuating devices of systems of space vehicles, for example, systems of adjustment of a form of a reflecting surface of a large-area reflector of the antenna or deployment mechanisms for a space telescope [6] a number of the requirements shown to the electric motor, such as: service life, efficiency, power consumption, torque, speed of rotation, model of external influencing factors, mass-size characteristics and others should be considered. With the optimal choice of electric motor, it is possible to ensure the reliable and efficient operation of both individual mechanical systems and the spacecraft as a whole.

Having analyzed the works [6] and [7], it was found that direct current motors (hereinafter – DCM) have proven to be a more versatile type of electric motors for space technology products due to their long service life, high torque and efficiency, relatively low heat generation, the ability to widely and smoothly regulate the speed of rotation, as well as small size and weight.

Let us consider the application of a DCM for tuning the radio-reflecting netting of a large-sized space-based reflector. Currently, research is actively underway to create these designs. [8], [9], [10], [11], [12], [13], [14], [15].

Fig. 1 shows the spoke 1, the two main radial cords of the rear 3 and front 2 networks and cables 4 going between them. At the right end of the spoke 1 is divided into two parts to set the desired shape of the radio-reflective surface. In each cable 4 is located actuator 5, which here is taken as a DC motor.

It is necessary, by adjusting the length of cables 4 with the help of actuators 5 to set the shape of the radio-reflective netting defined by the front net 2 while minimizing energy costs.

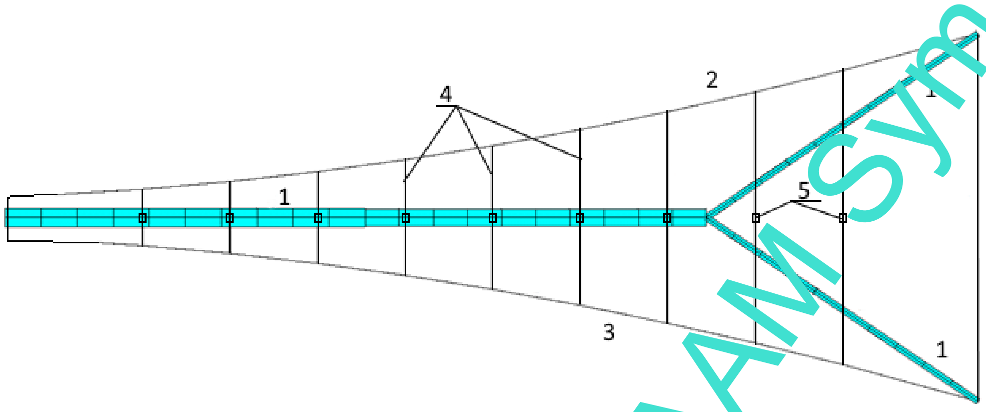

Fig. 1. Scheme of the space-based reflector spoke

Since the space-based reflector has a limited energy supply, the question of minimizing the energy cost to accomplish the tasks at hand arises separately. Currently, the control is performed by PID control structure, which allows achieving the required parameters in the terminal part. The application of optimal control algorithms will minimize energy costs. In addition, it is important to minimize the oscillation of the netting, this can be achieved by a smooth stop of the motor.

2. Building a mathematical model

The mathematical model must consist of electrical and mechanical parts [16], [17], [18], [19], described by equations to describe the DCM:

$$U = L \cdot \frac{dI(t)}{dt} + R \cdot I(t) + E(t), \quad (1)$$

$$M(t) - M_{ex} = J \cdot \frac{d\omega(t)}{dt}. \quad (2)$$

Equation (1) is a differential equation of electric equilibrium of the armature (rotor) motor circuit, where R is armature (rotor) active resistance, L is armature (rotor) winding inductance, $E(t)$ is counter EMF, $I(t)$ is motor current, U_a is armature (rotor) voltage. (1) does not consider the voltage drop (relatively small compared to the value of the rotor voltage), which nonlinearly depends on the rotor current, and assume that the armature (rotor) response is fully compensated, the excitation flux is constant, the active resistance of the armature circuit does not change during motor operation.

Equation (2) is the equation of mechanical equilibrium of the motor, where $M(t)$e is electromagnetic moment of the motor, M_{ex} is load resistance moment, J is rotor moment of inertia, $\omega(t)$ is angular velocity of the motor shaft. (2) does not consider the effect of frictional forces in the rotor rotation as they have a weak effect on the acceleration of the DCM shaft.

Let us describe each component (1) and (2) in more detail.

$$M(t) = k_M \cdot I(t), \quad (3)$$

where $M(t)$ is electromagnetic torque of the motor, k_M is motor torque constant, corresponding to the ratio between the torque developed by the motor and the current drawn, $I(t)$ is motor current.

$$E = k_E \cdot \omega(t), \quad (4)$$

where $E(t)$ is counter EMF, k_E is coefficient of proportionality, called back EMF constant, $\omega(t)$ is angular velocity of the motor shaft.

From (1) and (2) one can see that the speed of rotation of the motor shaft $\omega(t)$ is controlled by changing the armature (rotor) voltage.

Taking into account the above, as well as the fact that when using the DCM in the system of adjusting the shape of the large-sized reflector of the spacecraft antenna, it is necessary to control the angle of rotation of the engine shaft, the final system of differential equations of the DCM will take the following form $X = (I\ \omega\ \varphi)^T$ or in a piecemeal form:

$$\frac{dI(t)}{dt} = \frac{U_a - R \cdot I(t) - k_E \cdot \omega(t)}{L}, \tag{5}$$

$$\frac{d\omega(t)}{dt} = \frac{k_M \cdot I(t) - M_{ex}}{J}, \tag{6}$$

$$\frac{d\varphi(t)}{dt} = \omega(t). \tag{7}$$

DCM actuators of the system for adjusting the shape of the reflecting surface of the large-sized transforming reflector of the spacecraft antenna are often used as part of the gearmotor. As a first approximation, we will assume that the gear motor uses an instrumental gearbox with a gear ratio of $k_g = 1/i_g$, where i_g is the gear ratio of the instrumental gearbox.

The control task is to drive the DCM shaft from the initial position $X(0)$ to a given end state $X(t_f)$ under the control constraint, which is taken as the external supply voltage $U_a = \pm 12\ V$ for a given time t_f. This rotation angle φ_M will provide a change in the length of the cable.

3. Building a mathematical model

Various structures of proportional-integral-differential (PID)-controller, including those with control constraints, were considered as regulators.

The full vector of state variables X is available for measurement. Then the deviation of the vector from the set value $\Delta X = X_f - X(t)$, the integral $\int_0^t \Delta X dt$ and the derivative $\Delta\dot{X}$ are available for measurement and calculation. The PID controller generates control in the form of:

$$u = k_p \cdot \Delta X + k_i \cdot \int_0^t \Delta X dt + k_d \cdot \Delta\dot{X}, \tag{8}$$

where k_p, k_i, k_d are the proportional, integrating and differentiating gain components.

The application of the PID control structure does not consider the minimization of energy costs, which is important in conditions of energy limitation. Therefore, let us consider applications of the sequential optimization algorithm.

If for a system n of equations the optimization by a single objective functional solution leads to a two-point boundary value problem for a system of order $2n$, then for a hierarchy of two criteria this number is doubled [20]. It is possible to reduce the volume of calculations by using on two levels the functionals of the generalized work of A.A. Krasovsky [20] and [21]. The paper [20] shows the feasibility of a simplified version of the algorithm, when considering the second level of control of the first level is considered to be implemented. That is, there is a sequential optimization of controls by level. Studies for different systems have shown that the nature of the trajectories of controlled motion by the simplified algorithm does not change in comparison with the full solution [20]. The algorithm has been successfully used to control an aircraft, including the use of spiral prediction; to control a car, a nuclear reactor. Here the well-known advantages of applying the Krasovsky criterion remain, when instead of a two-point boundary value problem one has to solve two one-point Cauchy problems (in forward and backward time, respectively) [21].

Let us extend the system (5) - (7) by adding to it the equation $\dot{U}_a = u$. Assume $Y = U_a$, $x = (\mathrm{X}^T\ Y)^T = (I\ \omega\ \varphi)^T$, $f = (\mathrm{F}^T\ u)^T$. Consider a hierarchy of target functionals of the form

$$J_1 = V_{f1}(X, t_f), \tag{9}$$

$$J_2 = V_{f2}(X, t_f) + \int_{t_0}^{t_f} f_0(U_a, t)\, dt., \tag{10}$$

Here $V_f = 0{,}5\rho_1\left[I_a(t_f) - I_{af}\right] + 0{,}5\rho_2\left[\omega_M(t_f) - \omega_{Mf}\right] + 0{,}5\rho_3\left[\varphi_M(t_f) - \varphi_{Mf}\right]$, $f_0 = 0{,}5\left(\frac{U_a}{R}\right)^2$, where t_0 is the initial time, t_f is the final time, R is the resistance of the armature winding, ρ_1, ρ_2 are the given coefficients. Since the task was to minimize the energy cost, the expression for the consumed supply voltage U_a over the entire simulation interval was taken as a function f_0.

A simplified version of the algorithm is appropriate to control the electric motor with end conditions for the angle φ at small finite values of its derivative ω.

The control is calculated in the form $u = u_1 + u_2$, where u_1 and u_2 minimize the quality criteria $J_1$and J_2respectively. At the first level, the predictive model is adjusted, for example, so that it is possible to take $u_1 = 0$, $U_m(t) = U_a(t) + \Delta U_a$.

Taking into account the assumptions made, the Hamiltonian of the system (5) – (7) will take the form $H = P^T f(X) + f_0$, where $P = [P_I \; P_\omega \; P_\varphi \; P_U]$ is the vector of conjugate variables, or

$$H = P_\varphi \omega + P_\omega \frac{k_m \cdot I - M_{ex}}{J} + P_I \frac{U_a - R_a \cdot I_a - k_e \cdot \omega_M}{L} + P_U u + 0{,}5 \left(\frac{U_a}{R}\right)^2. \quad (11)$$

The equations of the predictive model at zero control [20] and [21] have the form

$$\dot{I} = \frac{U_a - R \cdot I(t) - k_E \cdot \omega(t)}{L}, \quad (12)$$

$$\dot{\omega} = \frac{k_M \cdot I(t) - M_{ex}}{J}, \quad (13)$$

$$\dot{\varphi} = \omega(t), \quad (14)$$

$$\dot{U_a} = 0. \quad (15)$$

Equations for conjugate variables are obtained by taking partial derivatives of equation (11) with a negative sign:

$$\dot{P_I} = -\frac{\partial H}{\partial I_a} = -P_\omega \frac{k_m}{J} + P_I \frac{R}{L}, \quad (16)$$

$$\dot{P_\omega} = -\frac{\partial H}{\partial \omega} = -P_\varphi + P_I \frac{k_e}{L}, \quad (17)$$

$$\dot{P_\varphi} = -\frac{\partial H}{\partial \varphi} = 0, \quad (18)$$

$$\dot{P_U} = -\frac{\partial H}{\partial U_a} = -P_I \frac{1}{L} - P_U - \frac{U_a}{R}. \quad (19)$$

The values of the conjugate variables at the final time t_f are determined from:

$$P_I(t_f) = \alpha_1[I(t_f) - I_f], \quad (20)$$

$$P_\omega(t_f) = \alpha_2[\omega(t_f) - \omega_f], \quad (21)$$

$$P_\varphi(t_f) = \alpha_3[\varphi(t_f) - \varphi_f], \quad (22)$$

$$P_U(t_f) = \alpha_4[U(t_f) - U_f]. \quad (23)$$

The value ΔU is chosen by iterating from the condition $V_{f1} = 0$ to the nearest small $\sigma > 0$ by integrating the equations of the first level model on the interval $[t, t_f]$. In this case, neglecting the friction moment on the predictive model, we can determine the control value required to minimize the first criterion in the model U_{md} from equation (6) in the form of $U_{md} = [\omega(t_f) - \omega_f/(t - t_f) \cdot A_d]$. Here $A_d = \frac{k_d L}{k_m}$, $k_d$is the additive coefficient.

To determine the control u_2 is required to find pu_2 only from the system of equations of the fitted model and the system of equations for p_2 at $V_{f1} = 0$. That is, set the value $u_1 = -k_1^2 p_{1U}$ in the form of $-k_1^2 p_{1U} = \delta(t)\Delta U$, where $\Delta U = U_{md} - U(t)$, $\delta(t)$ is a delta function. Approximately, we can take $\delta(t) = \frac{1}{\Delta t}$, where Δt is the step of numerical integration of the system (5) – (7).

The control is found from the condition $\frac{\partial H}{\partial U_a} = 0$, considering the limitation on the value of the control:

$$U_a = 12 \cdot sign(U_a). \quad (24)$$

4. Simulation

The data for the 0816K012SR series 0816SR electric motor from FAULHABER [22]. Let us simulate the system (5) – (7) using the developed optimal control algorithm and using a PID controller.

Consider the control problem of bringing the shaft of a servo motor from an initial position φ_0= 0 rad, ω_0= 0 rad/s, I_{a_0}= 0 A to a given final state φ_f= 8π rad, ω_f= 0 rad/s, I_{a_f}= 0 A in the absence of an external load M_{ex}= 0 for a time t_f= 1 s.

The simulation was performed by the Euler method with integration step h = 0.001. Application of a PID controller with coefficients k_p= 0.05, k_i= 0.002, k_d= 1.758 and an optimal controller with coefficients α_1= 1, α_2= 1, α_3= 14, α_4= 1, k_1= 0.32 showed identical results. Both algorithms successfully solved the problem. The error in fulfilling the terminal conditions for the angle of rotation of the motor rotor φ was not more than 0.0001 rad. The discrepancies in the total power input for control and the final shaft speed were insignificant and were caused by the choice of the integration method.

When the final angle of rotation of the rotor shaft is changed to φ_f = 160π rad (80 revolutions) and the coefficients are maintained, there is a deviation of the final speed ω from 0 when using PID controller (line 2 in Fig. 2a) in contrast to the optimal controller (line 1 in Fig. 2a). Due to the fact that in J_1 the condition of reaching ω = 0 at the finite moment of time is introduced, the optimization algorithm quickly reduces ω and at the last step of slow control brings it to the required value. The deviation of the final φ in both cases did not exceed 0.3 rad (Fig. 2b).

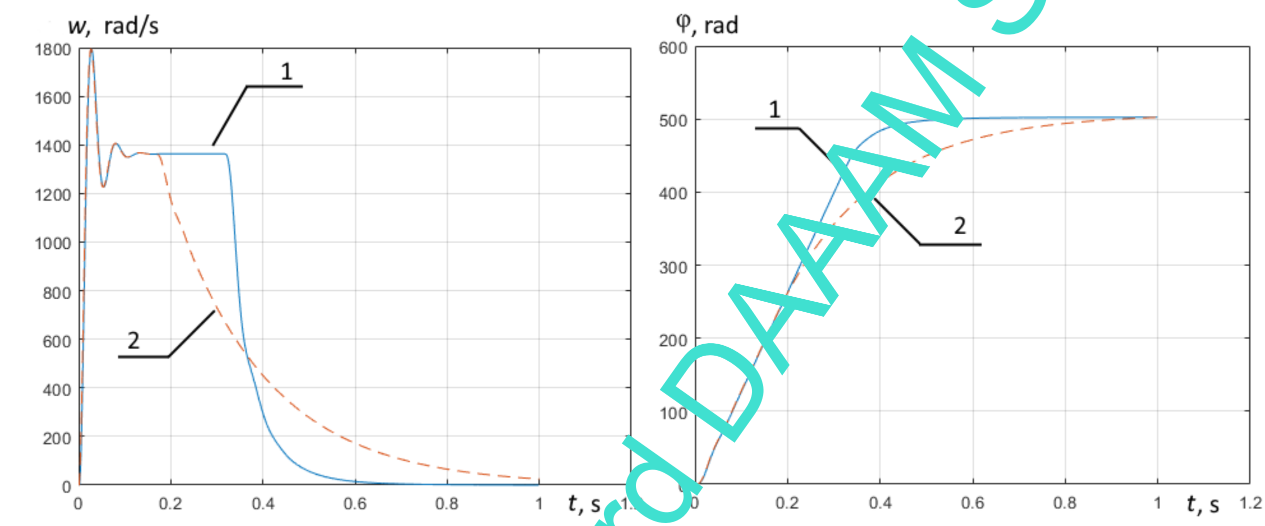

a) b)

Fig. 2. Transients diagram: a) $\omega(t)$, b) $\varphi(t)$, line 1 is a optimal controller, line 2 is a PID controller

Thus a PID controller requires adjustment of the coefficients. When the final angle of rotation of the rotor shaft is increased to φ_f = 250π rad (125 revolutions), adjustment of the coefficients is required for both types of regulators. A further increase in the final angle φ requires an increase in control time φ_f. Due to the absence of load on the rotor shaft, the power consumption does not differ significantly with different control options. The gain of the optimal regulator is ~1%.

Consider the application of the algorithms when torque M_{ex} = 0.61 mN·m and when setting the final rotor shaft angle of rotation φ_f = 200π rad (100 revolutions). Since the presence of torque leads to an increase in time, we assume t_f =1.5 s. The application of the PID controller with coefficients k_p = 1.1, k_i = 0.002, k_d = 1.3186 and the optimal controller with coefficients α_1 = 1, α_2 = 1, α_3 = 965, α_4 = 1, k_1 = 0.32 showed identical results. Both algorithms successfully solved the problem. The change in angular velocity ω is similar to the considered version without load. The PID control structure provides a smoother and longer variation in shaft speed. The optimum controller reduces the speed sharply and then slowly brings it to the desired value. This reduces the power consumption by ~13% from 1.0741 W to 0.9345 W when the optimum controller is used.

Fig. 3 shows graphs of the dependence $I(t)$ (line 1 is a optimal controller, line 2 is a PID controller). You can see that up to 1.1 s the control is at the limit (U = 12 V), then the current drops to 0 A. By changing the control of the optimum controller more quickly, the energy costs can be minimized.

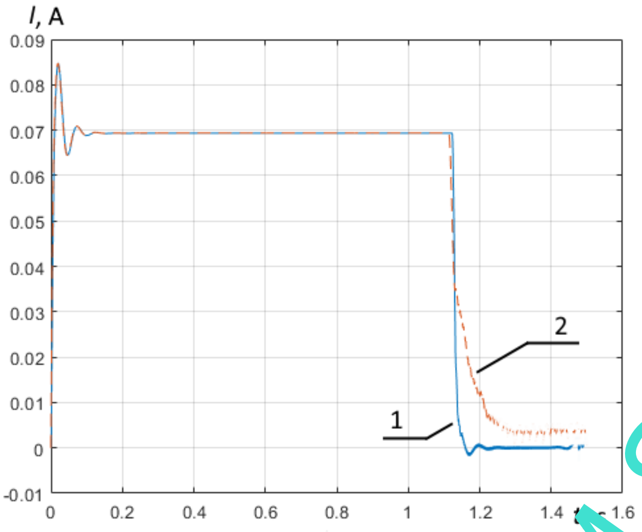

Fig. 3. Transients diagram $I(t)$, line 1 is a optimal controller, line 2 is a PID controller.

The selected coefficients allow us to successfully solve the problem in the range φ_f from 0 to 400π rad (200 revolutions).

As experience with finite-time control shows [23], it is possible to achieve the necessary accuracy and quality of regulation of the system in a wide range of terminal conditions. The proposed algorithm allows a real-time smooth approach to a given motor shaft speed. Taking into account the perturbations and noise of the assumed sensors acting on the system under study leads to complex problems of measurement result processing and planning [24] and [25].

5. Conclusion

The use of the algorithm of sequential optimization according to the hierarchy of criteria does not give a significant advantage over the PID controller when the regulation time is long enough. The reduction in energy costs was ~1%. However, in some cases it is possible to reduce the electrical costs with the optimal controller by ~13%.

The sequential optimization algorithm investigated in the article is reasonable to apply to more complex solutions using measurement processing and optimization of observation intervals. The results of these studies can be used to calculate the energy costs, the choice of actuator and the power plant of the space-based reflector.

In the future it is supposed to investigate the application of optimal control algorithms for a refined mathematical model of a direct current motor. Including an augmented gearbox model and a device that translates the angle of rotation of the motor shaft into changes in the length of the cable. It is also planned to consider the task of simultaneous control of several actuators for setting up and maintaining a given form of a radio-reflecting network drone, taking into account the optimization of finite time.

6. Acknowledgments

The study was supported by grant No. 22-79-10112 from the Russian Science Foundation, https://rscf.ru/en/project/22-79-10112/.

7. References

[1] Alekseev, K.B. & Bebenin, G.G. (1974). Control of space aircraft, - 2nd ed, Mashinostroenie, Moscow
[2] Dmitriev, V.S., Kostyuchenko, T.G. & Gladyshev, G.N. (2013). Electromechanical executive bodies of spacecraft orientation systems, Part I, Stipend studies, Publishing house of Tomsk Polytechnic University, Tomsk
[3] https://ie.rs-online.com/web/generalDisplay.html?id=ideas-and-advice/dc-motors-guide, (2022). Radionics Ltd. Official site, Everything You Need To Know About DC Motors, Accessed on: 2022-09-03
[4] Kankam, M.D. & Elbuluk, M.E. (2001). A Survey of Power Electronics. Applications in Aerospace Technologies, NASA/TM-2001-211298 IECEC2001-AT-32, Available from: https://ntrs.nasa.gov/api/citations/20020013943/downloads/20020013943.pdf Accessed: 2022.09.03
[5] https://ntrs.nasa.gov/api/citations/19750007247/downloads/19750007247.pdf Brushless DC Motors, Application of Aerospace Technology, NASA CR-2506, Accessed: 2022.09.03
[6] Tran, A. N. (2016). James Webb Space Telescope Deployment Brushless. DC Motor Characteristics Analysis, Proceedings of the 43rd Aerospace Mechanisms Symposium, 4-6 May 2016, NASA Ames Research Center,

Available from: https://ntrs.nasa.gov/api/citations/20160004038/downloads/20160004038.pdf Accessed: 2022.09.03

[7] https://extapps.ksc.nasa.gov/Reliability/Documents/Preferred_Practices/1229.pdf, Selection of Electric Motors for Space Applications, NASA Preferred Reliability Practices, Practice NO. PD-ED-1229, Accessed: 2022.09.03

[8] Yiqun, Z.; Na, L.; Guigeng, Y. & Wenrui, R. (2017). Dynamic analysis of the deployment for mesh reflector deployable antennas with the cable–net structure, Acta Astronautica, Vol. 131, pp 182–189, ISSN 0094-5765, DOI 10.1016/j.actaastro.2016.11.038

[9] Kabanov, S.A.; Krivushov, A.I. & Mitin, F.V. (2017). Modeling of joint deployment of units of the large-sized transformable reflector of space basing, SPIIRAS Proceedings, Vol.54, No 5, 2017, pp. 130-151, Print ISSN 2078-9181, Online ISSN 2078-9599, DOI: 10.15622/sp.54.6

[10] Mitin, F.; & Krivushov, A. (2017). Control deployment of mobile units of large-sized spacecraft, Proceedings of the 28th DAAAM International Symposium, pp. 0773-0779, B. Katalinic (Ed.), Published by DAAAM International, ISBN 978-3-902734-11-2, ISSN 1726-9679, Vienna, Austria, DOI: 10.2507/28th.daaam.proceedings109

[11] Ramachandran, S.; Neve, M. J. & Sowerby, K. W. (2018). Millimetre wave antenna deployment in a single room environment, IEEE Aerospace and Electronic Systems Magazine, Vol. 12., No. 15, pp. 23[illegible]-239[illegible], Print ISSN 1751-8725, Online ISSN 1751-8733, DOI: 10.1049/iet-map.2018.5512

[12] Rahmat-Samii, Y.; Manohar, V.; Kovitz, J. M. R. Hodges, Freebury, G. & Peral, E. (2019). Development of Highly Constrained 1 m Ka-Band Mesh Deployable Offset Reflector Antenna for Next Generation CubeSat Radars, IEEE Aerospace and Electronic Systems Magazine, Vol. 67, No. 10, pp. 6254-6266, ISSN: 0885-8985, DOI: 10.1109/TAP.2019.2920223

[13] Tserodze, S.; Prowald, J. S.; Chkhikvadze, K.; Nikoladze, M. & Muchadze, M. (2020). Latest modification of the deployable space reflector structure with V-folding bars, CEAS Space Journal: An Official Journal of the Council of European Aerospace Societies, Vol. 12, No. 2, pp. 163-169, Print ISSN 1868-2510, Online ISSN 1868-2502, DOI: 10.1007/s12567-019-0281-9

[14] Kabanov, S.A. & Mitin, F.V. (2020). Optimization of the stages of deploying a large-sized space-based reflector, Acta Astronautica, Special Issue on 6th SFS 2019, Vol. 176, pp. 717-724, ISSN 0094-5765, DOI: 10.1016/j.actaastro.2020.04.066

[15] Kabanov, S.A. & Mitin, F.V. (2021). Optimization of the Processes of Deployment and Shape Generation for a Transformable Space-Based Reflector, Journal of Computer and Systems Sciences International, Vol. 60, No. 2, pp. 283–302, Print ISSN 1064-2307, Online ISSN 1555-6530, DOI: 10.1134/S1064230720060052

[16] Petrov, U.P. (1971). Optimum control of the electric drive taking into account the limitations on heating, Energy, Leningrad

[17] Emelyanov A.A.; Beskletkin V.V.; Agzamov I.M.; Zozulin M.S.; Onishchenko K.Y.; Zorin D.I.; Blinov E.K.; Bukhryakov I.F.; Dyatlov O.A.; Chumichev P.E. & Shamiev R.R. (2019). Mathematical modeling of a DC motor in the system of relative units in Matlab and C, Young Scientist, Vol. 11 (249), pp. 1-7, ISSN 2077-8295.

[18] Pal, D. (2016). Modeling, Analysis and Design of a DC Motor based on State Space Approach, International Journal of Engineering Research & Technology (IJERT), Vol. 5 Issue 02, pp. 293-296, ISSN 2278-0181, DOI: 10.17577/IJERTV5IS020332

[19] Mitin, F. & Krivushov, A. (2018). Application of Optimal Control Algorithm for DC Motor, Proceedings of the 29th DAAAM International Symposium, pp. 0762-0766, B. Katalinic (Ed.), Published by DAAAM International, ISBN 978-3-902734-20-2, ISSN 1726-9679, Vienna, Austria, DOI: 10.2507/29th.daaam.proceedings110

[20] Kabanov, S.A. (1997). Control systems on predictive models, Publishing house of St. Petersburg State University, ISBN: 5-288-01941-X, St. Petersburg

[21] Krasovsky, A. A. (1987). Handbook on the theory of automatic control, Nauka, Moscow.

[22] https://www.faulhaber.com/en/products/series/0816sr/, (2022). FAULHABER GROUP Official site, FAULHABER SR Series 0816 ... SR, Accessed on: 2022-09-03

[23] Kabanov, S. A. & Mitin, F. V. (2021). Solution of the filtration problem with the optimal adjustment of the radio-reflecting net of a transformable reflector, Siberian Aerospace Journal, Vol. 22, No. 4, pp. 577–588, ISSN 2712-8970, DOI: 10.31772/2712-8970-2021-22-4-577-588

[24] Malyshev, V. V.; Krasilshchikov, M.N.; Bobronnikov, V.T.; Nesterenko, O.P. & Fedorov, A.V. (2000). Satellite monitoring systems, V. Malyshev (Ed.), Publishing House of Moscow Aviation Institute, ISBN: 5-7035-2384-2, Moscow

[25] Kabanov, S. A.; Kabanov, D. S.; Nikulin, E. N. & Mitin, F. V. (2021). Optimal control of deployment of the spoke of a transformable reflector in the presence of disturbance, Siberian Aerospace Journal, Vol. 22, No. 4, pp. 649–659, ISSN 2712-8970, DOI: 10.31772/2712-8970-2021-22-4-649-659